Threshold Selection with Relative J-Divergence for Image Segmentation

Fangyan Nie, *Member, IAENG,* and Pingfeng Zhang

Abstract—**As an image segmentation technique with high real-time performance, thresholding has been widely used in machine vision-based task processing. However, due to the complexity of application scenarios, different methods need to be designed for different task requirements. As an effective tool to measure the information distance between different information systems, relative J-divergence makes up for the deficiency of traditional information divergence. In this paper, a new image thresholding segmentation method is designed and implemented based on relative J-divergence. In the process of image segmentation, the optimal threshold is found based on the minimum relative J-divergence criterion. The optimal threshold is applied to separate the image pixels into two parts, namely target and background, so as to achieve the purpose of image segmentation. In the comparison with some classical algorithms, the proposed method is applied to the segmentation of nondestructive testing and other images. The experimental results verify the effectiveness, application prospects and popularize value of the proposed method.**

Index Terms—**image segmentation, histogram thresholding, information divergence, relative J-divergence.**

I. Introduction

IN many intelligent applications based on machine vision, image segmentation [1-2] is the underlying key technology to realize the entire intelligent components, such as industrial automation [3], medical auxiliary diagnosis [4-5], intelligent agriculture [6] and other production practice applications [7]. In the field of image segmentation, a kind of technology has been widely concerned in research and practical application. The technique is image thresholding segmentation technique. Image thresholding has become a very popular technology in image segmentation because of its simplicity in implementation, high real-time performance in application and good segmentation effect if the algorithm is properly selected for a specific task [8-10].

The most famous image thresholding segmentation algorithms include maximum between-class variance method [11], maximum entropy method [12], minimum error method [13], minimum cross entropy method [14], etc. Otsu [11] proposed the maximum between-class variance method. This method has been successfully applied in many fields and is also called Otsu method in various research literatures [15-18]. In this method, based on the histogram of image gray level, the author firstly classifies the image pixels into two categories by selecting one threshold, then constructs the between-class variance of the two categories, and finally determines the optimal threshold by finding the maximum value of between-class variance within the range of image gray level so as to achieve the purpose of image segmentation. The Otsu method has become one of the most well-known and widely used method due to its excellent performance. One of the shortcomings of Otsu method is that if the pixels' class distribution of image gray level histogram is not balanced, it is easy to cause the optimal threshold value to occupy the side with the dominant distribution [18]. The maximum entropy method [12] was proposed by Kapur et al. In this method, the histogram is regarded as the probability distribution of image gray level, and then the Shannon entropy is used to measure the amount of information in the image. The optimal threshold is obtained by maximizing the Shannon entropy in the image gray level interval. The maximum entropy method cleverly applies information theory to the field of image segmentation, and because of its excellent performance in the field of practical applications, the method has also gained rapid popularity since it was proposed [19]. The minimum error thresholding method was proposed by Kittler and Illingworth [13]. Based on the error analysis principle, a pixels' classification error criterion based on image histogram distribution is constructed, and then the optimal threshold is obtained by minimizing the criterion. The minimum cross entropy method was proposed by Li and Lee [14]. Similar to the maximum entropy method, the minimum cross entropy method also regards the gray level histogram distribution of the entire image as an information system. Then, the cross entropy is used to measure the information difference between the original image and the segmented image. Finally, the optimal threshold is obtained by minimizing cross entropy.

The above four methods have achieved great success in their respective application fields, and become the well-deserved typical representatives in the field of image thresholding segmentation technology. However, due to the defects of the criterion itself, these methods also have some insurmountable shortcomings, such as the unbalanced distribution threshold deviation problem in Otsu method [18], the meaningless problem of maximum entropy method and minimum cross entropy method when frequency distribution of some gray-levels in image histogram is 0, and the distribution fitting problem of minimum error thresholding method based on normal distribution [20]. Therefore, in order to overcome the shortcomings of these methods, many researchers have put forward many improvement schemes.

Relative J-divergence [21] is a new divergence measure proposed by Dragomir et al. Compared with traditional divergence measures (such as cross entropy), this measure can better measure the difference between different probability distributions, and makes up for some deficiencies in traditional divergence, so it has been widely used in many fields [22]. Image segmentation can be regarded as an

Manuscript received April 9, 2023; revised June 15, 2023.

This work is supported by the Natural Science Foundation of Hunan Province, China (Grant No.2021JJ50022).

Fangyan Nie is a professor of Computer and Information Engineering College, Guizhou University of Commerce, Guiyang 550014, China, (Corresponding author, e-mail: niefyan@gzcc.edu.cn).

Pingfeng Zhang is a lecturer of Marxism College, Guizhou University of Commerce, Guiyang 550014, China, (e-mail: 694069603@qq.com).

information measurement problem for image thresholding. Compared with the original image, if the loss of information of the segmented image is smaller, the segmentation effect should be better theoretically. Therefore, taking the relative J-divergence as the measurement tool of information loss in image segmentation, a new image threshold segmentation algorithm is proposed in this paper.

In the following, the Section 2 describes the basic theory and algorithm framework of the proposed method. The segmentation experiments and analysis are described in Section 3. The Section 4 summarizes and makes some concluding description.

II. Methodology of proposed method

A. Relative J-divergence

Divergences play an important role in the fields of pattern recognition, optimization, estimation, and neural computation etc. For two n-dimensional probability distributions $P = (p_1, p_2, \cdots, p_n)$ and $Q = (q_1, q_2, \cdots, q_n)$, the relative J-divergence is defined as follows.

$$D(P|Q) = \sum_{i=1}^{n} \left[(p_i - q_i) \log \left(\frac{p_i + q_i}{2q_i} \right) \right] \tag{1}$$

Divergence measures are commonly used to find a distance or difference between P and Q. Usually, the P corresponds to the observed data and the Q to estimated or expected data which are subject to constraints imposed on the assumed models.

B. The Proposed Thresholding Method

Based on the relative J-divergence, we proposed a new image threshold segmentation method. For a grey-level image I with size m×n, the implementation steps of the proposed method are described as follows.

Step 1: Count the number of gray levels of the image I, and represent it with $G = \{0, 1, 2, \cdots, L\}$. Here, L represents the maximum gray level of the image I. For 8-bit digital image, $L = 255$.

Step 2: Calculate the frequency probability of each gray level in the image I, and represent it with $h_i = n_i/(m \times n)$. Here, n_i represents the frequency of occurrence of the ith gray level in the image I. The frequency probability of the whole image I can be expressed by set $H = \{h_0, h_1, \cdots, h_L\}$.

Step 3: Assuming that t is a selected segmentation threshold, t divides G into two parts G_0 and G_1. Here, $G_0 = \{0, 1, \cdots, t\}$, and $G_1 = \{t+1, t+2, \cdots, L\}$.

Step 4: Calculate the sum of frequency probabilities P_0, P_1 about G_0 and G_1 with Equation 2.

$$P_0 = \sum_{i=0}^{t} h_i \quad , \quad P_1 = \sum_{i=t+1}^{L} h_i \tag{2}$$

Step 5: Calculate the image graylevel mean m_0 and m_1 about G_0 and G_1 based on Equation (3).

$$m_0 = \frac{1}{P_0} \sum_{i=0}^{t} (i \times h_i) \quad , \quad m_1 = \frac{1}{P_1} \sum_{i=t+1}^{L} (i \times h_i) \tag{3}$$

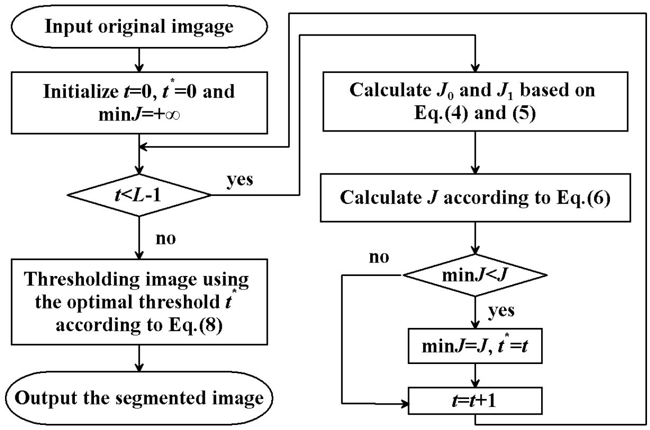

Fig. 1. The algorithm flow chart of the proposed method.

Step 6: Calculate the relative J-divergence J_0 and J_1 with respect to G_0 and G_1 using Equations 4 and 5.

$$J_0 = \sum_{i=0}^{t} \left\{ h_i \left[(i - m_0) \log \left(\frac{i + m_0}{2 \times m_0} \right) \right] \right\} \tag{4}$$

$$J_1 = \sum_{i=t+1}^{L} \left\{ h_i \left[(i - m_1) \log \left(\frac{i + m_1}{2 \times m_1} \right) \right] \right\} \tag{5}$$

Step 7: Define the criterion function for image thresholding segmentation with Equation 6.

$$J = J_0 + J_1 \tag{6}$$

Step 8: Search the optimal threshold t^* in G by Equation 7.

$$t^* = \arg \min_{t \in G} [J] \tag{7}$$

Step 9: If the image graylevel values of coordinates (x, y) of original image and segmented image are denoted by $f(x, y)$ and $s(x, y)$ respectively, the value of $s(x, y)$ can be determined by Equation 8 according to the optimal threshold t^*.

$$s(x,y) = \begin{cases} 0, & f(x,y) \le t^* \\ 255, & f(x,y) > t^* \end{cases} \tag{8}$$

Step 10: Output the result: the segmented image S.

In the proposed method, the relative J-divergence is used as the criterion function of the information loss of the segmented image relative to the original image. Theoretically, if the value of the criterion function is smaller, the quality of the segmented image is closer to the original image, and it should also be said that the segmentation quality is better.

C. Algorithm Flow diagram

In order to show the details of the proposed method more intuitively, here we use Figure 1 to describe the algorithm flow of the proposed method.

III. Experiments and analysis

To verify the effectiveness of the proposed method, the segmentation experiments are carried out in this Section. In experiments, the performance of the proposed method is compared with four famous methods mentioned above. The four methods are maximum between-class variance method presented by Otsu [11], maximum entropy method presented by Kapur et al. [12], minimum error thresholding method presented by Kittler and Illingworth [13], and minimum cross entropy method presented by Li and Lee [14]. In addition, an improved method based on the idea of Otsu's method [17] is also compared with the proposed method in this paper. For the convenience of description, here we refer to these methods as Otsu method, ME method, MET method, MCE method, IOtsu method, and the proposed method, respectively.

The above methods are all implemented by MATLAB programming language. The experimental environment is as follows.

Hardware environment: A laptop with Intel(R) Core (TM) i7-8550U CPU @1.80GHz 1.99 GHz and 16.0 GB RAM.

Software environment: 64-bit Windows 11 Home Chinese version operating system, MATLAB 7.10.0.499 (R2010a).

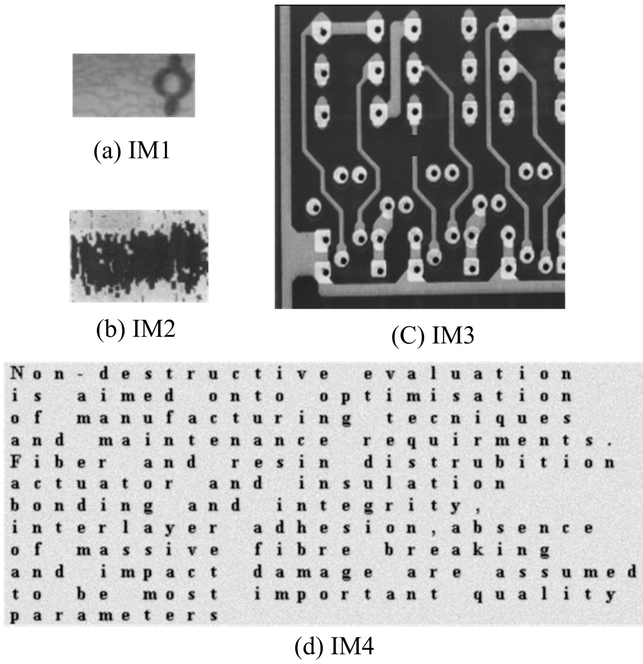

Fig. 2. The four original images for performance evaluation.

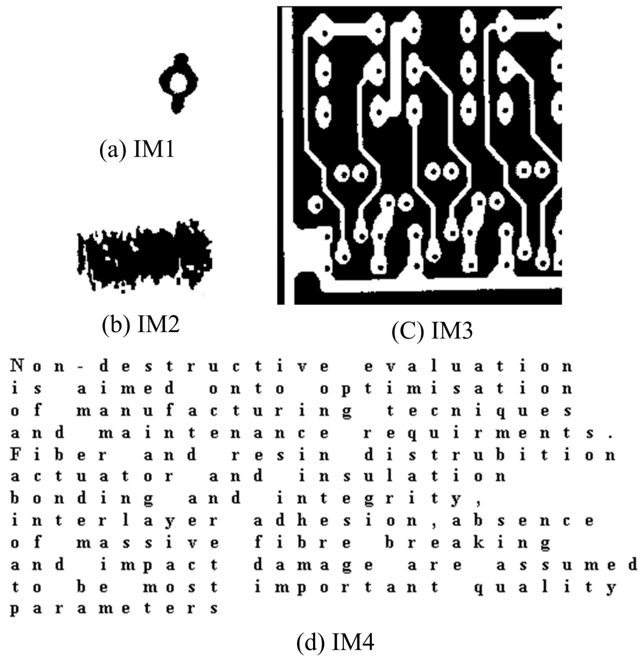

Fig. 3. The ground-truths of four test images.

A. Performance Evaluation

In experiments, we first carried out the performance comparison experiments. In the performance comparison experiments, we selected the images from reference [9] as the experimental images. The images from reference [9] not only contain the original images, but also the real segmented images manually segmented by experts. Therefore, these images are very suitable for the performance evaluation of image segmentation algorithm. These images have been used in many literatures.

Here, four images are selected for the performance evaluation experiments. The four images are shown in Figure 2. For the convenience of narration, these four images are referred to as IM1, IM2, IM3, and IM4, respectively. IM1 and IM2 are two nondestructive testing images of workpieces with defects. IM3 is a printed circuit board (PCB) image for nondestructive testing. IM4 is a is contaminated document image. Figure 3 shows the real segmented images by experts, i.e., the ground-truths of images in Figure 2. The sizes of these images are 51×98, 74×111, 243×232, and 227×551, respectively.

Figure 4 lists the gray-level histograms of these four images. As can be seen from Figure 4, the gray-level frequency distributions of these images are very uneven, with unimodal, bimodal and multimodal distributions. It is not a simple task to separate the background and the target of the image by finding a suitable threshold.

Figures 5-8 show the segmentation results of these four images. Figure 5 shows the result of image IM1. As can be seen from Figure 5, the segmentation result of MET method is the worst. The proposed method and the MCE method have better segmentation results than the other three methods. The MET method does not separate the image object from the background at all. The residual noise pixels in the segmentation results of Otsu method, ME method and IOtsu method are more than those of the proposed method and MCE method.

Figure 6 shows the result of image IM2. It can be seen from Figure 6 that the edges of the segmentation results obtained by the MET method, the MCE method and the proposed method are relatively smooth, while the edges of the results obtained by the Otsu method, the ME method and the IOtsu method have some residual noise pixels.

Figure 7 shows the result of image IM3. Visually, in Figure 7, the ME method basically does not effectively separate the target, and the results obtained by other methods are basically similar, and they all separate the target.

Figure 8 shows the result of image IM4. In Figure 8, the

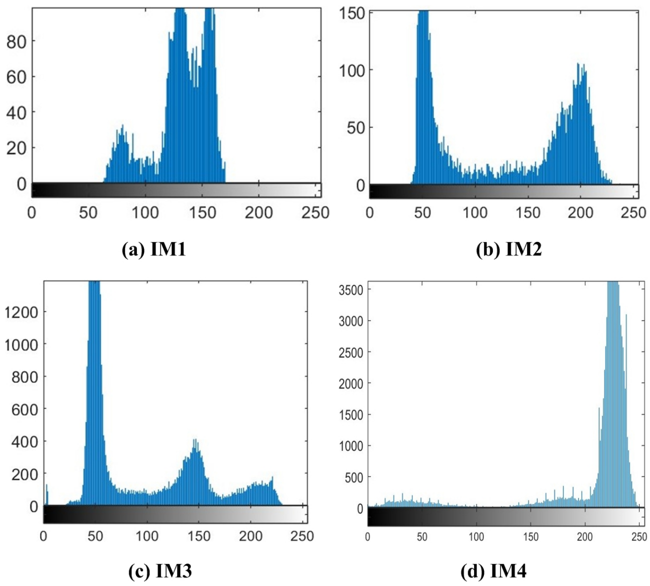

(a) IM1 (b) IM2 (c) IM3 (d) IM4

Fig. 4. The histograms of test images.

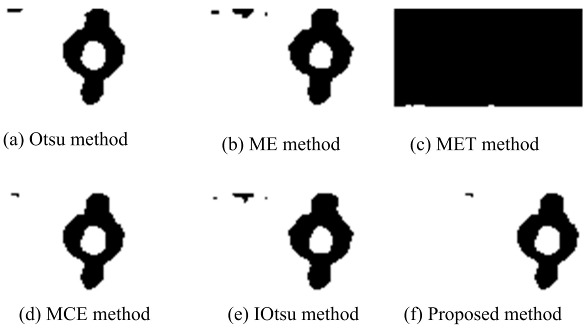

(a) Otsu method (b) ME method (c) MET method (d) MCE method (e) IOtsu method (f) Proposed method

Fig. 5. The segmented results of image IM1 by 6 different methods.

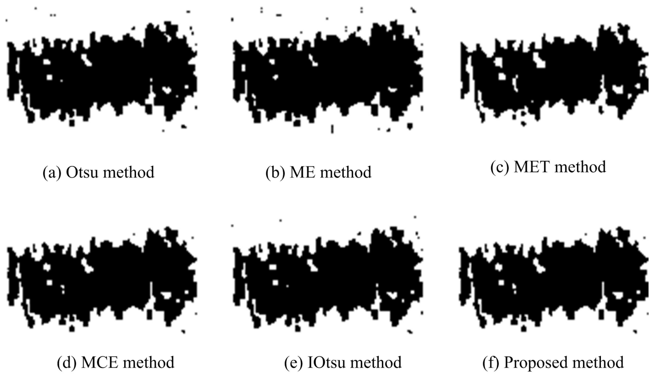

(a) Otsu method (b) ME method (c) MET method (d) MCE method (e) IOtsu method (f) Proposed method

Fig. 6. The segmented results of image IM2 by 6 different methods.

results obtained by the ME method, MET method and IOtsu method are vague, while the results obtained by the Otsu method, MCE method and proposed method are clear and the characters can be distinguished.

Table 1 lists the optimal thresholds obtained by each method when segmenting test images. As can be seen from Table 1, the optimal thresholds obtained by IOtsu method are similar to that obtained by Otsu method, and the threshold obtained by the proposed method are similar to that obtained by MCE method. The Otsu method and IOtsu method are based on the theory of between-class variance, and the MCE method and proposed method are based on the divergence theory. Therefore, it is not surprising that the results obtained by these methods are similar from theoretical source, which also verifies the effectiveness of the proposed method from another aspect.

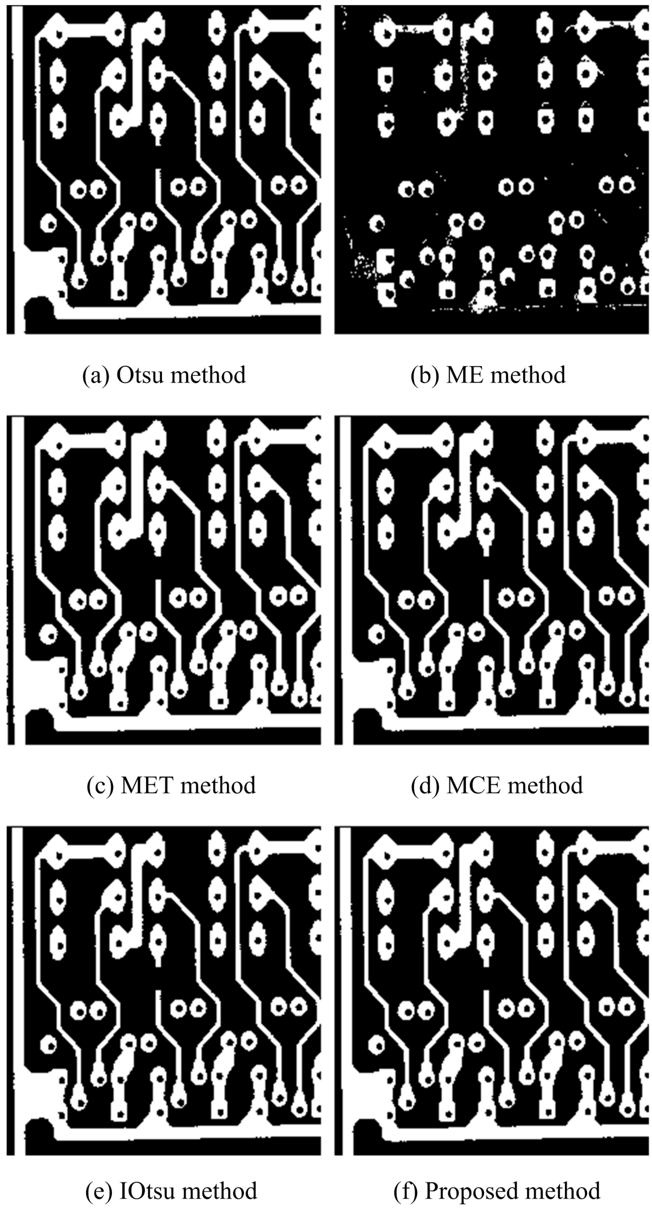

(a) Otsu method (b) ME method (c) MET method (d) MCE method (e) IOtsu method (f) Proposed method

Fig. 7. The segmented results of image IM3 by 6 different methods.

TABLE I
THE OPTIMAL THRESHOLDS OF TEST IMAGES OBTAINED BY 6 METHODS.

Method	IM1	IM2	IM3	IM4
Otsu method	113	123	106	136
ME method	117	139	155	171
MET method	169	78	68	203
MCE method	110	108	94	111
IOtsu method	116	118	100	168
Proposed method	110	107	93	110

Table 2 lists the time performance comparison for each method. As can be seen from Table 2, the proposed method did not take more than 0.02 seconds for the segmentation of image IM4 with the largest size 227×551 in the test images. Compared with the Otsu method, the time-consuming of the

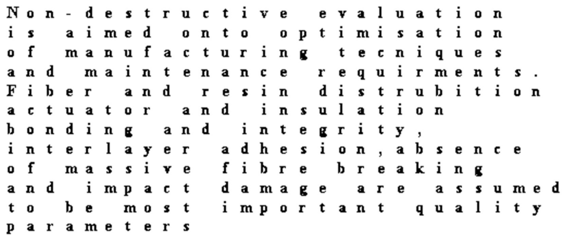

(a) Otsu method

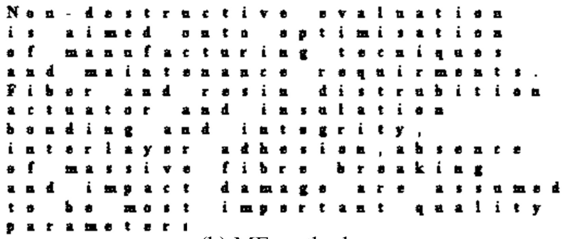

(b) ME method

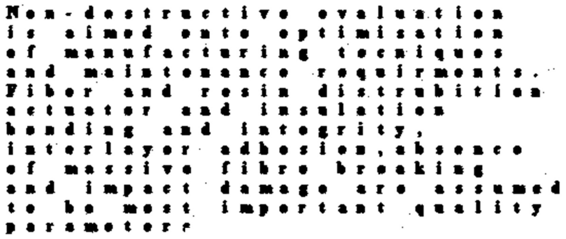

(c) MET method

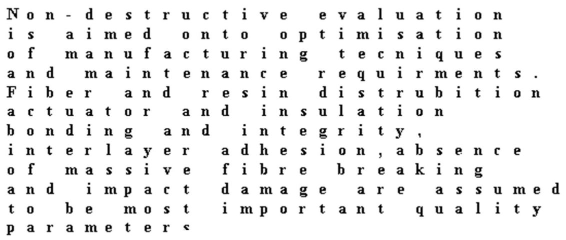

(d) MCE method

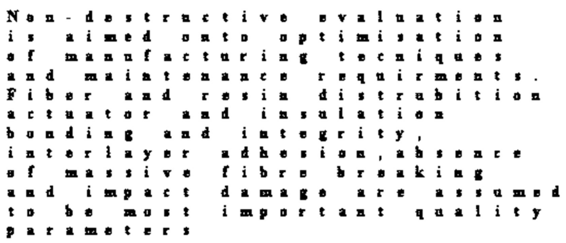

(e) IOtsu method

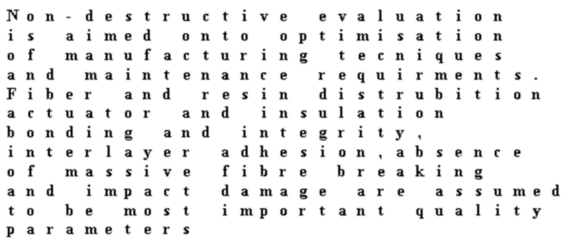

(f) Proposed method

Fig. 8. The segmented results of image IM4 by 6 different methods.

proposed method is about one-fifth of the time-consuming of the Otsu method. Therefore, in terms of time performance, the proposed method has good popularization and application value.

TABLE II
THE PERFORMANCE COMPARISON OF CALCULATION TIME (SECOND).

Method	IM1	IM2	IM3	IM4
Otsu method	0.0346	0.0477	0.0743	0.1106
ME method	0.0121	0.0209	0.0326	0.0464
MET method	0.0071	0.0093	0.0113	0.0148
MCE method	0.0075	0.0101	0.0128	0.0154
IOtsu method	0.0095	0.0149	0.0164	0.0207
Proposed method	0.0077	0.0113	0.0128	0.0150

TABLE III
THE COMPARISON OF *NTPM* FOR EACH METHOD.

Method	IM1	IM2	IM3	IM4
Otsu method	0	0	0	0
ME method	0	0	0	0
MET method	0	297	1317	0
MCE method	0	0	0	21
IOtsu method	0	0	0	0
Proposed method	0	0	0	24

TABLE IV
THE COMPARISON OF *NBPM* FOR EACH METHOD.

Method	IM1	IM2	IM3	IM4
Otsu method	98	237	2016	587
ME method	192	458	12305	3683
MET method	4291	0	68	9037
MCE method	67	78	1072	86
IOtsu method	164	199	1588	3319
Proposed method	67	70	999	76

The analysis of segmentation results in Figures 5-8 are all qualitative analysis based on visual discrimination. In order to describe the performance of each method more objectively, the results of each method will be analyzed quantitatively below. In order to facilitate the analysis, we first define the following parameter variables.

TNMP: The total number of misclassified pixels.

NTPM: The number of target pixels that are misclassified.

NBPM: The number of background pixels that are misclassified.

TNPI: The total number of pixels in the image.

RMP: The ratio of misclassified pixels in the image.

Where, *TNMP* = *NTPM* + *NBPM*; *TNPI* = $m \times n$, $m \times n$ is the size of image; *RMP* = *TNMP* / *TNPI*. For *TNMP*, *NTPM*, *NBPM*, and *RMP*, the smaller their values, the better the performance of the segmentation algorithm.

Tables 3-5 show the statistical data of *NTPM*, *NBPM* and *RMP* respectively.

It can be seen from Table 3 that the MET method misclassifies more target pixels on images IM2 and IM3. The MCE method and the proposed method misclassify a few target pixels on image IM4.

As can be seen from Table 4, the Otsu method on image IM3, ME method on images IM3 and IM4, MET method on images IM1 and IM4, MCE and the proposed methods on image IM3, IOtsu method on images IM3 and IM4, more background pixels are misclassified.

From Table 3 and 4, the performance of the proposed method is generally better than other methods on the test

TABLE V
THE COMPARISON OF *RMP* FOR EACH METHOD.

Method	IM1	IM2	IM3	IM4
Otsu method	0.0196	0.0289	0.0358	0.0047
ME method	0.0384	0.0558	0.2183	0.0294
MET method	0.8585	0.0362	0.0246	0.0723
MCE method	0.0134	0.0095	0.0190	0.0009
IOtsu method	0.0328	0.0242	0.0282	0.0265
Proposed method	0.0134	0.0085	0.0177	0.0008

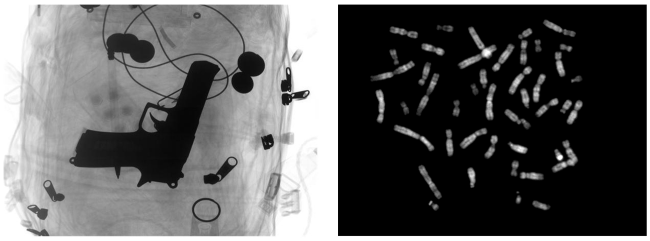

(a) X-ray image **(b) Chromosome image**

Fig. 9. The original images for testing.

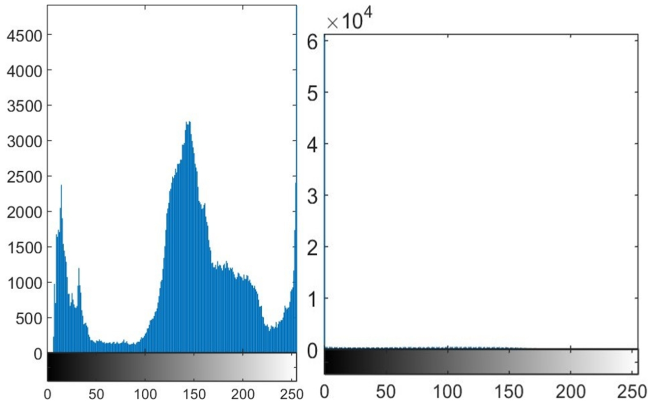

(a) X-ray image **(b) Chromosome image**

Fig. 10. The histograms of test images.

images, which can also be seen from Table 5. In Table 5, the values of *RMP* of the proposed method are all smaller than those of other methods.

B. Experiments on Other Images

To better verify the effectiveness of the proposed method, another experiments are conducted on other types of images. Here, an X-ray image [23] for security check and a human chromosome image [4] for karyotype analysis are selected for testing.

The two original images are shown in Figure 9, and their histograms are shown in Figure 10. The size of X-ray image is 452×612, the size of chromosome image is 576×768.

As can be seen from Figures 9 and 10, for the X-ray image, the gray level of its target pixels is mainly concentrated in the low value range, and the amount of target pixels accounts for a small proportion of the whole image, which can be seen from Figure 10 (a). For chromosome image, its target pixels account for a small proportion of the total pixels of the whole image, and the background pixels account for a large proportion, which are mainly distributed at and near 0 gray level.

TABLE VI
THE OPTIMAL THRESHOLDS OBTAINED BY EACH METHOD.

Method	X-ray image	Chromosome image
Otsu method	102	60
ME method	119	16
MET method	254	0
MCE method	76	13
IOtsu method	112	58
Proposed method	74	11

TABLE VII
THE COMPUTING TIME OF DIFFERENT METHODS (SECOND).

Method	X-ray image	Chromosome image
Otsu method	0.2910	0.5637
ME method	0.0981	0.2759
MET method	0.0164	0.0181
MCE method	0.0178	0.0203
IOtsu method	0.0222	0.0225
Proposed method	0.0180	0.0209

Table 6 shows the optimal thresholds obtained by each method for segmentation of X-ray image and chromosome image. Table 7 shows the computing time of each method on segmentation of X-ray image and chromosome image.

As can be seen from Table 6, the optimal thresholds obtained by the proposed method and MCE method conform to the above analysis. The thresholds obtained by the MET method are a little extreme. The thresholds obtained by Otsu methods and IOtsu method are slightly biased towards the dominant distribution of gray level, and the thresholds obtained by ME method are somewhat similar to that obtained by Otsu method.

From the calculation time of each method in Table 7, the time performance advantage of the proposed method is also more prominent, which meets the requirements of high real-time tasks.

Figures 11 and 12 show the segmentation results of each method on X-ray image and chromosome image. For the X-ray image, the segmentation result obtained by MET method is the worst, and there are more noise pixels left in the results obtained by ME method and IOtsu method. The Otsu method, MCE method and the proposed method obtain better results. For the chromosome image, the Otsu method and IOtsu method are a bit over-segmented, while the MET method is a bit under-segmented. For the ME method, MCE method and the proposed method, they obtain better segmentation results. For these two images, the results obtained by the proposed method are smoother in comparison.

IV. CONCLUSION

Image segmentation plays a very important role in machine vision-based image processing tasks. Due to the complexity of various task scenarios, appropriate segmentation algorithms are required to meet the task requirements under different conditions. In this paper, an image threshold segmentation method based on relative J-divergence is proposed.

Compared with some classical image threshold segmentation algorithms, the performance of the proposed method is investigated on the segmentation of nondestructive testing

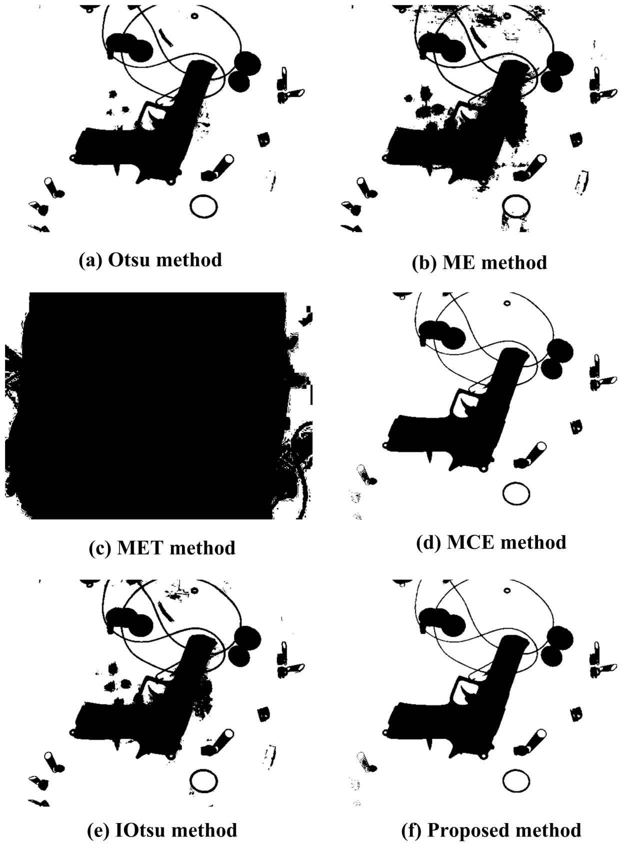

Fig. 11. The segmented results of X-ray image.

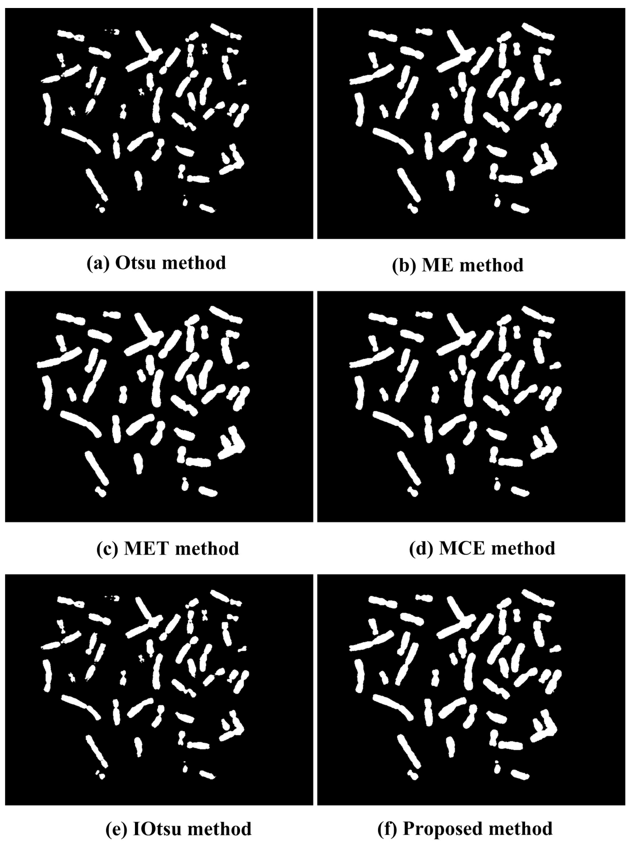

Fig. 12. The segmented results of chromosome image.

images, degraded document images, X-ray images for security check and human chromosome images for karyotype analysis. On the basis of the above experiments, the performance of the proposed method is analyzed qualitatively and quantitatively.

Experimental results show that the proposed method has good segmentation performance and less computation time. The performance of the proposed method is better than or similar to that of the classical threshold segmentation algorithms. This also shows that the proposed method has a good value of promotion and application.

At present, we only investigate the segmentation performance of the proposed method on gray image. The real world is rich and colorful. In the future, we will also apply the proposed method to color image segmentation and analyze its performance.

REFERENCES

[1] X. X. Yuan, and Y. Xu, "Salient object detection based on improved PoolNet," *Engineering Letters*, vol. 30, no.4, pp.1558-1565, 2022.

[2] P. Mesejo, Ó. Ibáñez, Ó. Cordón, and S. Cagnoni, "A survey on image segmentation using metaheuristic-based deformable models: state of the art and critical analysis," *Applied Soft Computing*, vol. 44, pp. 1-29, 2016.

[3] C. Ge, J. Wang, J. Y. Wang, Q. Qi, H. Sun, and J. Liao, "Towards automatic visual inspection: A weakly supervised learning method for industrial applicable object detection," *Computers in Industry*, vol. 121, pp. 103232, 2020.

[4] E. Poletti, F. Zappelli, A. Ruggeri, and E. Grisan, "A review of thresholding strategies applied to human chromosome segmentation," *Computer Methods and Programs in Biomedicine*, vol. 108, no. 2, pp. 679-688, 2012.

[5] Mousami Turuk, R. Sreemathy, Sadhvika Kadiyala, Sakshi Kotecha, and Vaishnavi Kulkarni, "CNN based deep learning approach for automatic malaria parasite detection," *IAENG International Journal of Computer Science*, vol. 49, no.3, pp.745-753, 2022.

[6] L. C. Ngugi, M. Abelwahab, and M. Abo-Zahhad, "Tomato leaf segmentation algorithms for mobile phone applications using deep learning," *Computers and Electronics in Agriculture*, vol. 178, pp. 105788, 2020.

[7] I. Kotaridis, and M. Lazaridou, "Remote sensing image segmentation advances: A meta-analysis," *ISPRS Journal of Photogrammetry and Remote Sensing*, vol. 173, pp. 309-322, 2021.

[8] P. K. Sahoo, S. Soltani, and A. K. C. Wong, "A survey of thresholding techniques," *Computer Vision, Graphics, and Image Processing*, vol. 41, no. 2, pp. 233-260, 1988.

[9] M. Sezgin, and B. Sankur, "Survey over image thresholding techniques and quantitative performance evaluation," *Journal of Electronic Imaging*, vol. 13, no. 1, pp146-165, 2004.

[10] N. Kheradmandi, and V. Mehranfar, "A critical review and comparative study on image segmentation-based techniques for pavement crack detection," *Construction and Building Materials*, vol. 321, pp. 126162, 2022.

[11] N. Otsu, "A threshold selection method from gray-level histograms," *IEEE Transactions on Systems, Man, and Cybernetics*, vol. 9, no.1, pp62-66, 1979.

[12] J.N. Kapur, P.K. Sahoo, and A.K.C. Wong, "A new method for gray-level picture thresholding using the entropy of the histogram," *Computer Vision, Graphics, and Image Processing*, vol. 29, no. 3, pp.273-285, 1985.

[13] J. Kittler, and J. Illingworth, "Minimum error thresholding," *Pattern Recognition*, vol. 19, no. 1, pp.41-47, 1986.

[14] C.H. Li, and C.K. Lee, "Minimum cross entropy thresholding," *Pattern Recognition*, vol. 26, no. 4, pp.617-625, 1993.

[15] T. Y. Goh, S. N. Basah, H. Yazid, M. J. A. Safar, and F. S. A. Saad, "Performance analysis of image thresholding: Otsu technique," *Measurement*, vol. 114, pp. 298-307, 2018.

[16] P. D. Sathya, R. Kalyani, and V. P. Sakthivel, "Color image segmentation using Kapur, Otsu and Minimum Cross Entropy functions based on Exchange Market Algorithm," *Expert Systems with Applications*, vol. 172, pp. 114636, 2021.

[17] H. Cai, Z. Yang, X. Cao, W. Xia, and X. Xu, "A new iterative triclass thresholding technique in image segmentation," *IEEE Transactions on Image Processing*, vol. 23, no. 3, pp. 1038-1046, 2014.

[18] X. Xu, S. Xu, L. Jin, and E. Song, "Characteristic analysis of Otsu threshold and its applications," *Pattern Recognition Letters*, vol. 32, no. 7, pp. 956-961, 2011.

[19] D. Zhao, L. Liu, F. Yu, A. A. Heidari, M. Wang, G. Liang, K. Muhammad, and H. Chen, "Chaotic random spare ant colony optimization for multi-threshold image segmentation of 2D Kapur entropy," *Knowledge-Based Systems*, vol. 216, pp. 106510, 2021.
[20] J. Xue, and Y. Zhang, "Ridler and Calvard's, Kittler and Illingworth's and Otsu's methods for image thresholding," *Pattern Recognition Letters*, vol. 33, no. 6, pp. 793-797, 2012.
[21] S. S. Dragomir, V. Gluevi, and C. E. M. Pearce, "Approximations for Csiszár f-divergence via midpoint inequalities," *Inequality theory and applications*, vol. 1, pp. 139-154, 2001.
[22] P. Kumar, and I. J. Taneja, "Generalized relative J-divergence measure and properties," *International Journal of Contemporary Mathematical Sciences*, vol. 1, no. 13, pp. 597-609, 2006.
[23] D. Mery, V. Riffo, U. Zscherpel, G. Mondragón, I. Lillo, I. Zuccar, H. Lobel, M. Carrasco, "GDXray: The database of X-ray images for nondestructive testing," *Journal of Nondestructive Evaluation*, vol. 34, pp. 42, 2015.

Fangyan Nie received his Ph.D degree in instrument science and technology from the Chongqing University, Chongqing, China, in 2010. Currently, he is a professor at the Computer and Information Engineering College, Guizhou University of Commerce, China, and a Researcher of Hunan Provincial Key Laboratory of Distributed Electric Propulsion Vehicle Control Technology, Changde, Hunan 415000 China. His research interests include image processing, machine vision, deep learning and swarm intelligence optimization algorithm.